JOURNAL OF AIRCRAFT
Vol. 47, No. 3, May–June 2010

Identification and Attenuation of a Tonal-Noise Source on an Aircraft's Landing Gear

Yong Li,* Malcolm G. Smith,† and Xin Zhang‡
University of Southampton, Southampton, England SO17 1BJ, United Kingdom

DOI: 10.2514/1.43183

Aircraft landing gear noise is a major contributor to the overall airframe noise during the landing approach of a commercial aircraft. Fairings covering geometrically complex areas of the gears have proved to be very effective in noise reduction. However, in tests on an A340's main landing gear, the overall benefit of the fairings was offset by both a slight increase in low-frequency broadband noise and a strong tonal noise. In this study, the identification and attenuation of the tonal-noise source has been carried out using a one-quarter-scale A340 main-landing-gear model. Aeroacoustic and aerodynamic tests were conducted in a closed-section wind tunnel, using a phased microphone array on the ceiling of the test section, flush-mounted pressure transducers on the model surface, and the particle-image-velocimetry technique. Far-field noise tests were then taken in an open jet aeroacoustic facility, using far-field microphones to verify the wind-tunnel test results. The experiments demonstrated the tonal-noise mechanism and a number of different control methods.

Nomenclature

a	=	leading-edge gap distance
C_0	=	speed of sound
D	=	characteristic length
f	=	frequency
f_d	=	cavity driving frequency
L	=	door-cavity length
L_m	=	surface-pressure-fluctuation level
L_n	=	normalized surface-pressure-fluctuation level
U, V, W	=	velocity components in Cartesian coordinates
U_{ref}	=	reference wind speed
U_∞	=	freestream wind speed
X, Y, Z	=	Cartesian coordinates
Φ	=	polar angle of the polar array
Ψ	=	polar angle of the traversing ring array
Ω_z	=	spanwise vorticity

I. Introduction

AIRFRAME noise can be equal to or louder than engine noise during the approach-to-landing phase of an aircraft, especially when the aircraft is equipped with modern high-bypass-ratio engines [1,2]. With the growth of air traffic around the world, the annoyance near airports is increasing, and the environmental concerns and noise certification regulations make the study of airframe noise an important research topic.

One of the major sources of airframe noise is known to be the landing-gear noise, which has been observed in full-scale wind-tunnel and flight tests, using acoustic mirror/array and far-field microphones [3–5]. In general, the landing-gear noise is dominated by broadband noise components due to the complexity of the geometry. Within the European Union research projects RAIN (reduction of airframe and installation noise) and SILENCER (significantly lower community exposure to aircraft noise), fairings were designed to cover noisy areas of the landing gear on an A340 aircraft, and a good level of noise reduction was achieved relative to the unmodified landing gear. However, in both full-scale wind-tunnel and flight tests [3,4], there was a drop in noise-reduction performance of the fairings in the 500–800 Hz frequency range (630 Hz at a one-third-octave band frequency) because of a new tonal-noise source. It was thought that this effect was likely to be caused by the main landing gear, which has larger-sized fairings, or possibly from the leg-door filler fairing or side-stay fairing. The objective of the work described in this paper was to identify the source of this tonal noise and investigate various methods of control.

A one-quarter-scale model of A340 main landing gear with fairings was used for the investigation. Initial measurements were carried out in a conventional closed-section wind tunnel, using a phased microphone array and surface-mounted microphones to localize the new noise source and the laser particle-image-velocimetry (PIV) technique for aerodynamic measurements. Final tests to verify the results from the wind tunnel were then conducted in an open jet aeroacoustic facility, using far-field microphones.

II. Description of Experiments

A. Test Model

The one-quarter-scale model of the A340 main landing gear installed in the wind tunnel is shown in Fig. 1a with the leg door, the hinge door, and the drag stay labeled, as these components are particularly relevant to this study. The leg-door filler fairing covers the gap between the leg door and the drag stay. On the aircraft, the main landing-gear leg is laterally inclined by 12.8 deg with respect to the wing's lower surface; therefore, in the test setup, a corresponding angle of 77.2 deg is realized between the gear leg and the tunnel sidewall. The bogie axis on the gear model is orientated 35 deg toe up with reference to the gear leg. A Cartesian coordinate system is also defined with the X coordinate in the streamwise direction.

B. Wind-Tunnel Test Setup

Aerodynamic and aeroacoustic measurements were performed in the 2.1×1.7 m closed-section wind tunnel at the University of Southampton, shown in Fig. 1b. A sidewall arrangement for the gear with a wall cavity was used to simulate the in-flight geometric/aerodynamic environment of the gear under the wing of the aircraft. The blockage of the wind tunnel was about 10%, based on the model frontal area, and the tunnel speed was measured by a pitot-static tube positioned well upstream of the gear. The freestream turbulence intensity was approximately 0.2% over the velocity range, up to the

Received 12 January 2009; revision received 18 January 2010; accepted for publication 14 February 2010.

*Research Fellow, Airbus Noise Technology Centre; y.li@soton.ac.uk. Member AIAA.
†Technical Manager, Institute of Sound and Vibration Research; mgs@isvr.soton.ac.uk.
‡Professor, Airbus Noise Technology Centre; x.zhang1@soton.ac.uk. Associate Fellow AIAA.

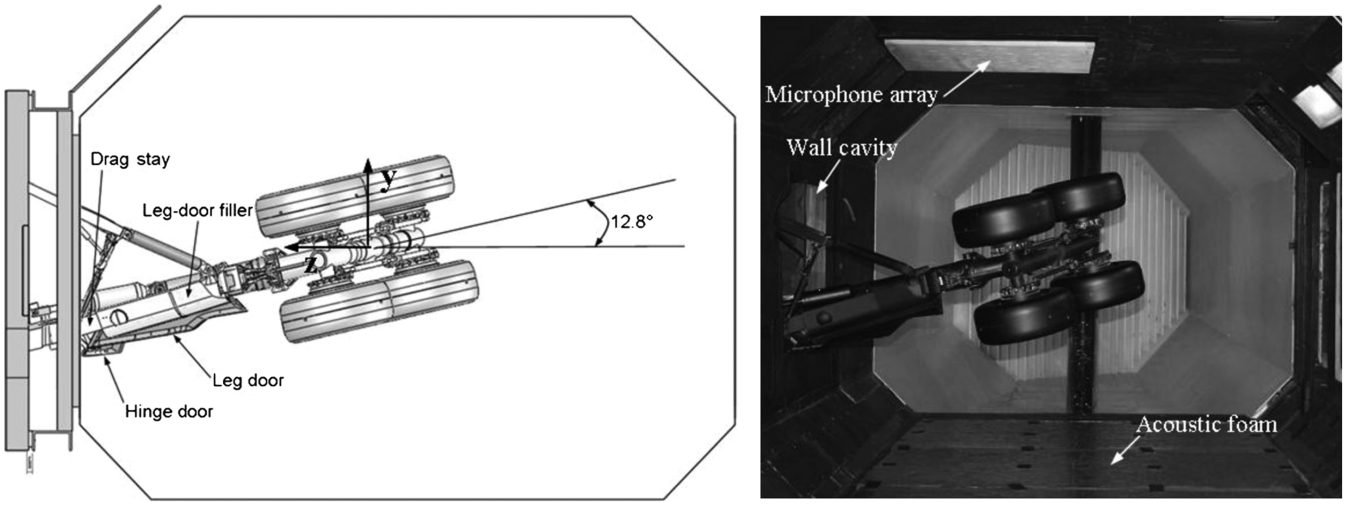

a) b)

Fig. 1 Wind-tunnel test setup with the gear model installed: a) schematic of front view showing the corresponding installation and details of the model and b) overview in the wind tunnel.

maximum wind speed of $U_\infty = 45$ m/s. Most of the tests were performed at a wind speed of 40 m/s, which is about half of the actual aircraft approaching speed, so that Strouhal numbers for the landing-gear noise are approximately half the values of those for the full-scale flight.

1. Phased Microphone Array Measurements

Two major challenges for noise measurements in this type of wind tunnel are the high background noise levels and the reverberant sound field, so that measurements using individual microphones are of little use. One solution to this problem is to use the beamforming technique [6], in which a phased array of microphones flush-mounted on the wall surface of the test section is used to produce noise-source maps for different frequencies. This technique suppresses uncorrelated pressure fluctuations on the microphones, mainly caused by the turbulence in the wind-tunnel boundary layer, and it also helps to suppress background noise propagating up the wind tunnel and acoustic images of the gear in the wall of the tunnel. The floor of the test section was also lined with 25 mm of acoustic foam to further reduce the effect of acoustic image sources, especially at higher frequencies in which sidelobes in the array sensitivity might cause problems.

A multiarm log spiral design [7] of the array was employed because of its good suppression of sidelobes at high frequencies. The phased microphone array was mounted on the ceiling of the test section to localize the noise sources along the length of the gear from the side-view direction, as shown in Fig. 1b. The array consisted of 56 flush-mounted Panasonic WM-60A electrets condenser microphones, which were covered by a smooth woven cloth material to reduce the effect of boundary-layer noise. Each microphone was calibrated using a reference Brüel and Kjær microphone, that was positioned adjacent to each array microphone in turn, and a point source of white noise on the floor of the test section. The transfer function from the reference microphone to the array microphone gave a frequency-dependent amplitude correction for each microphone.

The data were sampled at 48 kHz and analyzed using a block size of 4096, yielding a frequency resolution of about 12 Hz. To reduce spectral leakage, a Hanning window function was applied to each single block before performing the fast Fourier transform, and a total of 100 blocks were averaged to achieve the required statistical confidence. Details of the postprocessing of the data, based on conventional frequency-domain beamforming using a fully populated matrix of cross-spectral components with the autospectral elements suppressed, can be found in Fenech and Takeda [8]. Although the noise at each individual microphone was dominated by extraneous pressure fluctuations, such as those due to the wind-tunnel boundary-layer turbulence (despite the cloth covering), it was found that excellent images of the noise sources on the landing gear could still be obtained using this well-established array technique. The scan plane on the landing-gear leg was about 0.75 m from the microphone array, and the power spectrum for the complete scan plane was calculated at a number of frequencies within each one-third-octave frequency band of interest.

The error of the beamforming plots is not particularly important, because they are only used for a comparison between configurations. But a rough estimate can be obtained from two wind-tunnel runs with an identical configuration, which gives a maximum uncertainty of 1.5 dB for the beamforming noise map.

2. Onsurface Microphone Measurements

The gear also had 20 flush-mounted microphones, the same type as those used in the phased array, installed on the surface of the gear model to record the local surface-pressure fluctuations. However, only data from microphones P19 and P20, which were mounted on the lower surface of the leg door (as shown in Fig. 2), are presented here, as these are the most relevant to the tonal-noise problem. Microphone P19 is located near the leading edge of the leg door, whereas P20 is situated near the trailing edge of the door. Both microphones are positioned in the cavity between the leg door and the hinge door. The data processing was the same as for the phased array microphones, except that only the autospectra are used.

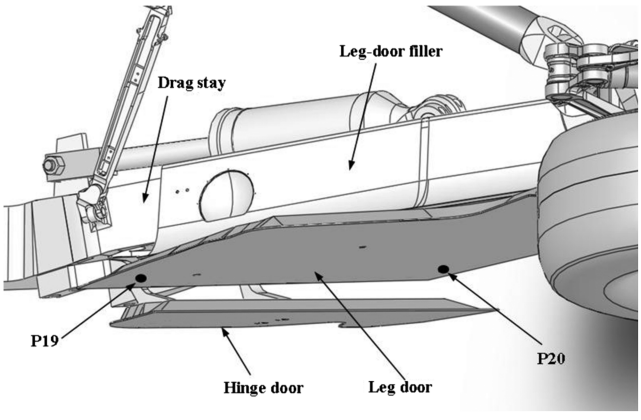

Fig. 2 Positions of onsurface microphones P19 (near the leg-door leading edge) and P20 (near the leg-door trailing edge.).

3. Particle Image Velocimetry Measurements

The laser PIV technique was used to visualize the local flow structure in the open cavity between the leg door and the hinge door, although it was difficult to set up the equipment because of the complex geometry in that area and because the cavity was very close to the wind-tunnel wall. To illuminate the area, the laser had to be installed upstream of the landing gear. So, to avoid changing the flow conditions in front of the landing gear, the laser box had to be positioned outside the wind tunnel, and a small slot was cut in the wind-tunnel sidewall to provide optical access. As a result, the laser sheet was angled at about 8 deg from the flow direction, as shown in the sketch in Fig. 3.

The PIV system was a Dantec dynamics system with a New Wave Gemini neodymium-doped yttrium–aluminum-garnet dual laser and a Dantec HiSense 1024×1280 resolution charge-coupled-device camera. The camera was set up perpendicular to the laser sheet and fixed on a support structure installed on the floor of the test section; this was sufficiently far from the gear-leg door that the flow in that area was unaffected. A total of 250 images of the flowfield were taken for each experimental condition, and each image set was processed using a 32×32 pixel cross-correction area and a $50 \times 50\%$ overlap to improve the resolution of the vector map. Spurious vectors on the map were then further removed using a range validation, whereby vectors greater than a specified magnitude would be rejected.

The accuracy of the instantaneous velocity fields can be estimated by assuming an accuracy in the correlation of 0.1 pixel displacement [9], which corresponds to a maximum error in the velocity of 0.4 m/s. When using a multisample, as described by Moffat [10], the uncertainty in a time-averaged vector is 0.02 m/s.

C. Far-Field Noise Test Setup

For the final validation tests, far-field noise measurements were performed in the QinetiQ Noise Test Facility (NTF) in Farnborough, U.K. The NTF is a large anechoic chamber with internal dimensions of $27 \times 26 \times 15$ m, which is effectively anechoic down to a frequency of 90 Hz, making it suitable for far-field noise measurements over a wide frequency range. The facility is normally used for model-scale jet-noise research, and these tests made use of the 1.8-m-diam jet that is used for the flight simulation in jet-noise experiments. The facility is capable of flow velocities up to 110 m/s, although measurements of the landing-gear noise were only made at 40, 62, and 78 m/s.

The landing gear was mounted in the undercarriage cavity of a dummy wing, which was positioned partially inside the nozzle of the NTF, as shown in Fig. 4. The gear was located about 1.8 m from the nozzle exit, fully inside the core flow of the jet, and the downstream edge of the dummy wing was serrated to minimize noise radiation from the edge. The assembly datum was such that, when installed, the main support leg was horizontal, representing the flyover configuration to a polar array of microphones in the horizontal plane. This was accomplished by rotating the dummy-wing assembly by about 12.8 deg from vertical.

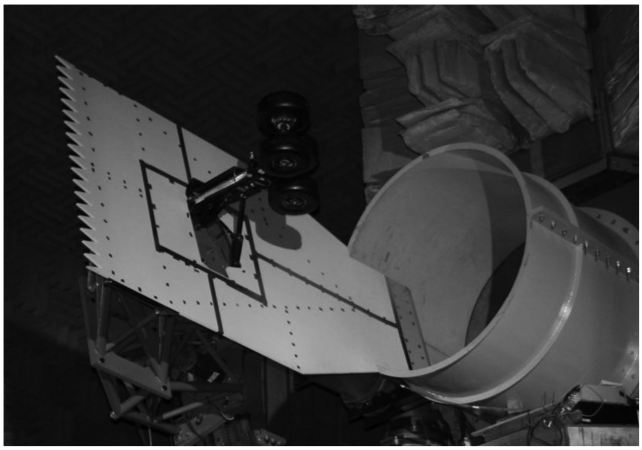

Fig. 4 NTF noise test setup, with main landing gear installed.

Noise measurements were made using two far-field microphone arrays. The first was a polar array, which was positioned in the same horizontal plane as the model at a distance of approximately 12 m, comprising nine one-quarter-inch normal-incidence microphones at 10 deg intervals, from $\Phi = 60$ deg (identified as microphone P60) to $\Phi = 140$ deg (P140) with respect to the aircraft axis, corresponding to 120–40 deg with respect to the jet axis in the NTF. The second array was a 12-m-diam ring of microphones that could be traversed axially to provide azimuthal information at nine axial locations with nominal polar angles of $\Psi = 70$–150 deg in 10 deg steps with respect to the aircraft axis, although the array was located at polar angle $\Psi = 150$ deg for most of the tests. The azimuthal microphone lying closest to plane of the polar array had an actual azimuthal angle of 91 deg (microphone R91). Here, Φ and Ψ represent the polar angles of the polar array and the traversing ring array, respectively, as shown in Fig. 5.

The noise data were acquired for 18 s, using a 32 channel Datmax system sampling at 200 kHz. The acquisition time was chosen to provide statistically satisfactory data in the lowest one-third-octave frequency band of interest (200 Hz for this model-scale gear). To effectively use the full dynamic range of the measurement equipment, in the frequency range of interest, the Nexus amplifiers were set to the highest high-pass filter setting of 20 Hz to suppress the effect of low-frequency pressure oscillations in the facility. All noise data acquired during testing were processed using the QinetiQ noise analysis program NanSy V5.0. This software provides data in a fully

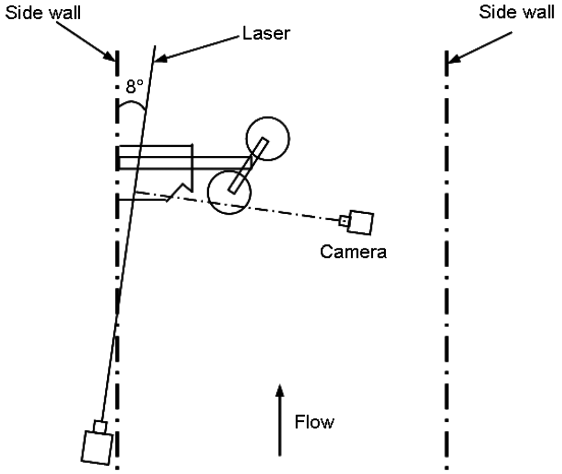

Fig. 3 Schematic of the PIV measurement setup in the wind-tunnel test section (not to scale). View is from the ceiling of the wind-tunnel test section.

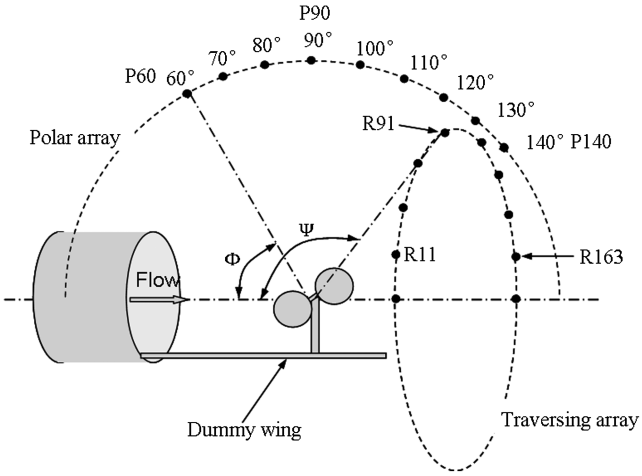

Fig. 5 Microphone positions and definition of radiation angles of the two microphone arrays from the top-view direction (not to scale).

corrected form and includes the shift in polar angle and level correction (shear-layer corrections [11]) that are required to present the data as if they were from an aircraft in flight in a stationary medium.

The processing of the data from onsurface microphones P19 and P20 was the same as the test in the closed-section wind tunnel.

III. Experimental Results and Discussions

This section summarizes a series of tests using the measurement methods on the landing-gear model as previously described. The possible tonal-noise mechanism and the control treatments to reduce the noise level are also discussed here.

A. Tonal-Noise Identification

The first requirement of the tests was to localize the tonal-noise source and to identify the mechanism. However, with the initial installation of the landing gear in its baseline configuration (same as the full-scale and flight tests), no tone was detected. Tonal sources are often sensitive to the precise flow conditions, and it was found that rotating the whole gear just a few degrees in the wind tunnel (corresponding to the yaw angle of the aircraft) was sufficient to generate a strong tone at 1450 Hz at a wind speed of 40 m/s. The level of the tone increased when the gear was rotated to a negative yaw angle relative to the flow direction, corresponding to a toe-out orientation of the gear on an aircraft, whereas a positive yaw angle did not generate the tone. A yaw angle of −3 deg was selected for further investigation of noise mechanism and control strategies. Although it was found that the leg-door filler fairing was effective in reducing the broadband noise in the area behind the drag stay due to the flow blockage, this fairing could also strengthen the tonal noise, which can be shown later.

The microphone array indicated that the noise source was located in the area around the leading edges of the leg door and the hinge door. Figure 6 shows noise maps for the one-third-octave frequency band centered at 1450 Hz. The scan plane was about 0.75 m from the microphone array surface, and the dash–circle line indicates the edge of the array on the scan plane. The origin of the Cartesian coordinates here is on the center of the array surface. In the gear baseline configuration, it was hard to identify the tonal-noise source, as indicated in Fig. 6a, but when the leg-door filler fairing was installed (Fig. 1a), the noise source near the leading areas of the leg door and the hinge door gained strength, shown in Fig. 6b. This was mainly due to the blockage of the leg-door filler fairing that forced the fluid to flow over the entrance of the cavity between the leg door and the hinge door. However, the tone was still not audible because of the strong wind-tunnel background noise. When the landing gear was rotated to a yaw angle of −3 deg, a very strong tonal noise could be detected (Fig. 6c), and the tone was even audible outside the wind tunnel, despite the high background noise.

Figure 7 shows, for the three different configurations, the power spectra of surface-pressure-fluctuation signals L_m for microphones P19 and P20 and also for one of the microphones in the array. In the baseline configuration without rotation (Fig. 7a), the signal is completely broadband, with no tonal noise at any of the three

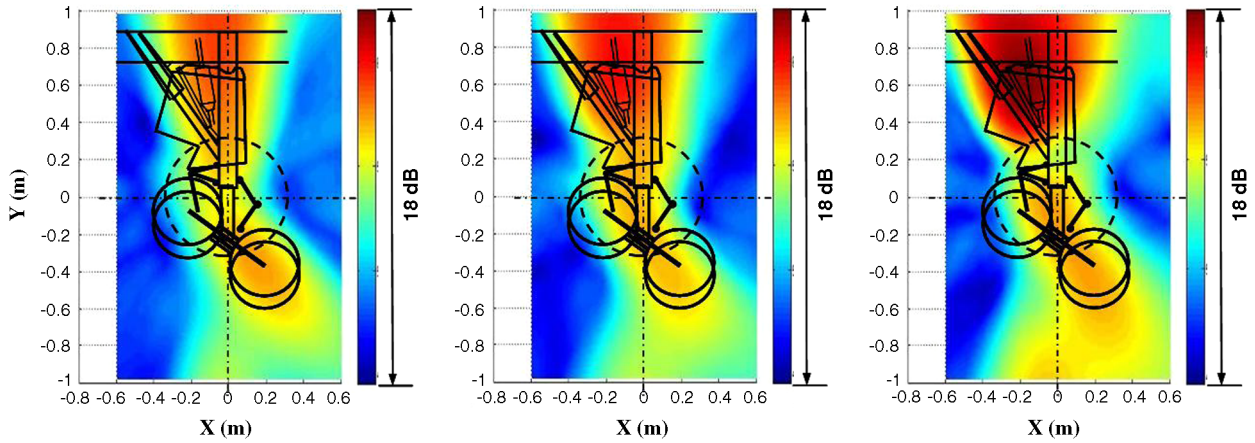

Fig. 6 Noise source map in a one-third-octave frequency band centered at 1450 Hz: a) baseline configuration, without rotation; b) plus leg-door filler, without rotation; and c) plus leg-door filler, with −3 deg rotation. Flow is from left to right.

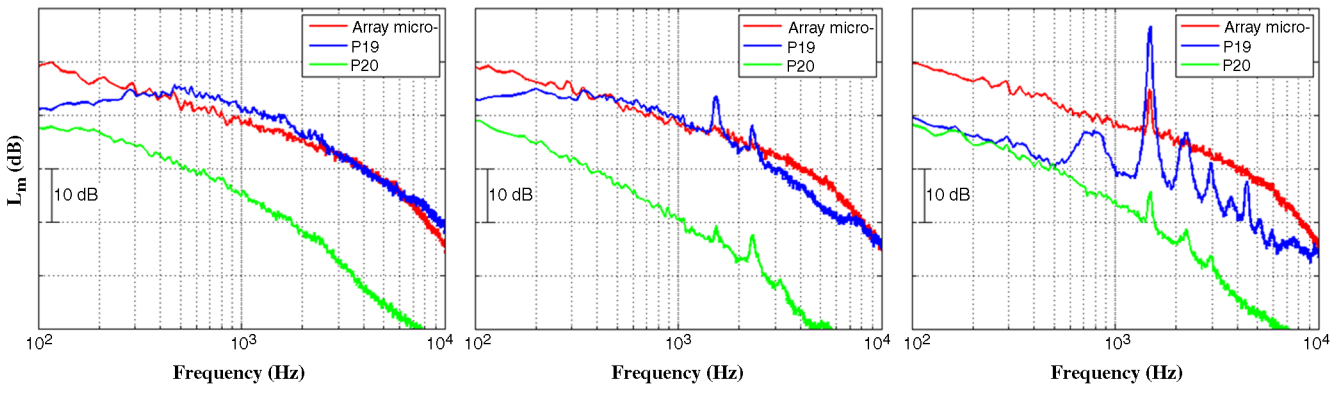

Fig. 7 Power spectra of surface-pressure fluctuations (dB, re: 20 μ Pa) at measurement points P19 and P20 and one of the array microphones with a wind speed of 40 m/s: a) baseline configuration, without rotation; b) plus leg-door filler, without rotation; and c) plus leg-door filler, with −3 deg rotation.

measurement points. With the leg-door filler fairing installed (Fig. 7b), two tones appear in the spectra of P19 and P20, indicating that the altered local flow conditions caused by the installation of the leg-door filler fairing is starting to excite the resonance, although the tone was not strong enough to be detected by the array microphone because of the high level of boundary-layer noise. Finally, applying the yaw angle of −3 deg (Fig. 7c), the power spectrum of P19 is dominated by harmonic series peaks, narrow band rather than fully tonal, dominated by 1450 Hz. There is a broad spectral peak at nominally 725 Hz, and the other peaks are harmonics of this fundamental frequency, with 1450 Hz being the first harmonic. The strength of the narrow band source at 1450 Hz is such that it is even apparent at the microphone array.

The effect of flow speed on the tonal noise is shown in Fig. 8. The dominant frequencies are 725 Hz for a wind speed of 20 m/s, 1000 Hz for 27 m/s, and 1450 Hz for 40 m/s, and the peak level increases rapidly with flow speed. In each case, the peak occurs at the first harmonic frequencies of a spectral hump at 360, 500, and 725 Hz, respectively. In Fig. 8b, the spectra have been based on a level-vs-speed dependence according to a U^4 power law ($L_n = L_m - 40\log(U/U_{\text{ref}})$, where L_n is the normalized power spectrum of the surface-pressure fluctuation, $U_{\text{ref}} = 40$ m/s, and Strouhal number ($St = fD/U$, where f is the frequency and D is the characteristic length). A U^4 power law has been used here, because this is the expected power law for near-field turbulence. In accordance with previous work [3] in which a characteristic length of 1 m was used as the reference length scale for a full-scale landing gear (roughly corresponding to one wheel diameter), in this case, a value of $D = 0.25$ m was chosen to represent this one-quarter-scale gear model. The first peak in the pressure fluctuations occurs at a Strouhal number of 4.75, and the dominant narrow band frequency at the first harmonic occurs at a Strouhal number of about 9.5 for all three test speeds. However, the higher harmonics slightly shift to a lower Strouhal number as the wind speed increases. The constant Strouhal number of the dominant peak indicates that the driving mechanism for the noise must be linked to a vortex shedding process.

B. Tonal-Noise Generation Mechanism

The data in Figs. 6–8 indicate that the tonal noise is associated with the flow over the entrance to the open cavity between the leg door and the hinge door, the local geometry being presented schematically in Fig. 9. The theoretical driving frequency for an aeroacoustic feedback mechanism in the leading-edge gap is [12]

$$f_d = 1/(a/U + a/C_0)$$

where a is the distance between the two leading edges (approximately 50 mm), C_0 is the sound speed, and U is the mean flow speed. This frequency corresponds to the time taken for a vortex to be convected across the gap and an acoustic wave to propagate back. Taking $C_0 = 340$ m/s and the mean velocity $U = 40$ m/s gives a predicted driving frequency of approximately 715 Hz,

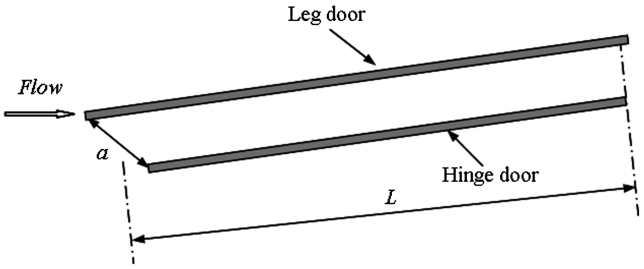

Fig. 9 Schematic of the model, simulating the open cavity between the leg door and the hinge door.

roughly in accordance with the frequency of the spectrum hump at about 725 Hz in Fig. 7c.

Considering the cavity as an open-ended pipe, the longitudinal resonances can be expressed approximately as [13]

$$f_n = \frac{n}{2 \times (L/C_0)}; \qquad n = 1, 2, 3, \ldots$$

The length of the cavity L is about 355 mm, and this gives resonant frequencies of 480, 960, 1440, 1920, 2400, ... , N Hz.

Taking the fundamental driving frequency of the vortex shedding as 725 Hz, with harmonics of the driving frequencies at 1450, 2175, ... , N Hz, it can be seen that, within the accuracy of the formula, the first harmonic driving frequency of 1450 Hz is coincident with the third-cavity resonance at 1440 Hz. This helps to drive the vortex feedback mechanism at the leading edge of the cavity, which results in the observed strong tone at a wind speed of 40 m/s. At the two lower wind speeds of 20 and 27 m/s, the first harmonic frequencies (725 and 1000 Hz, respectively) of the noise generated at the leading edge are not harmonically related to the resonance frequency of the cavity, and no strong resonance occurs. The normalized level at 40 m/s is about 20 dB higher than for 20 m/s, whereas the U^4 power law would suggest a change of 12 dB. This indicates that the longitudinal resonance of the cavity between the leg door and the hinge door plays an important role in enhancing the noise level.

The tonal noise is thus considered to be caused by a combination of the aeroacoustic feedback mechanism in the gap between the leading edges of the two doors and the acoustic resonance in the open-ended cavity.

C. Tonal-Noise Control

Having identified the source mechanism of the tonal noise, the next task was to find practical ways of suppressing it. The following five treatments, shown in Fig. 10, were selected in the wind-tunnel tests: 1) serrated spoiler attached on the leg-door leading edge, 2) soft puttylike material (Plasticene) covering the hinge-door leading edge, 3) vortex generators attached to the lower surface of the leg-door leading edge, 4) hinge door rotated 30 deg relative to the leg door, and 5) hinge-door removal (not shown in Fig. 10).

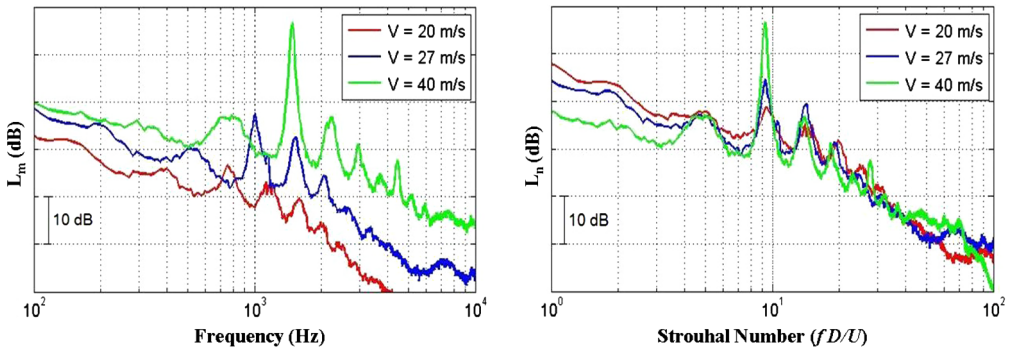

Fig. 8 Effect of speed on narrowband noise power spectra recorded by the leading-edge microphone P19: a) wall pressure level vs frequency and b) normalized wall pressure level vs Strouhal number.

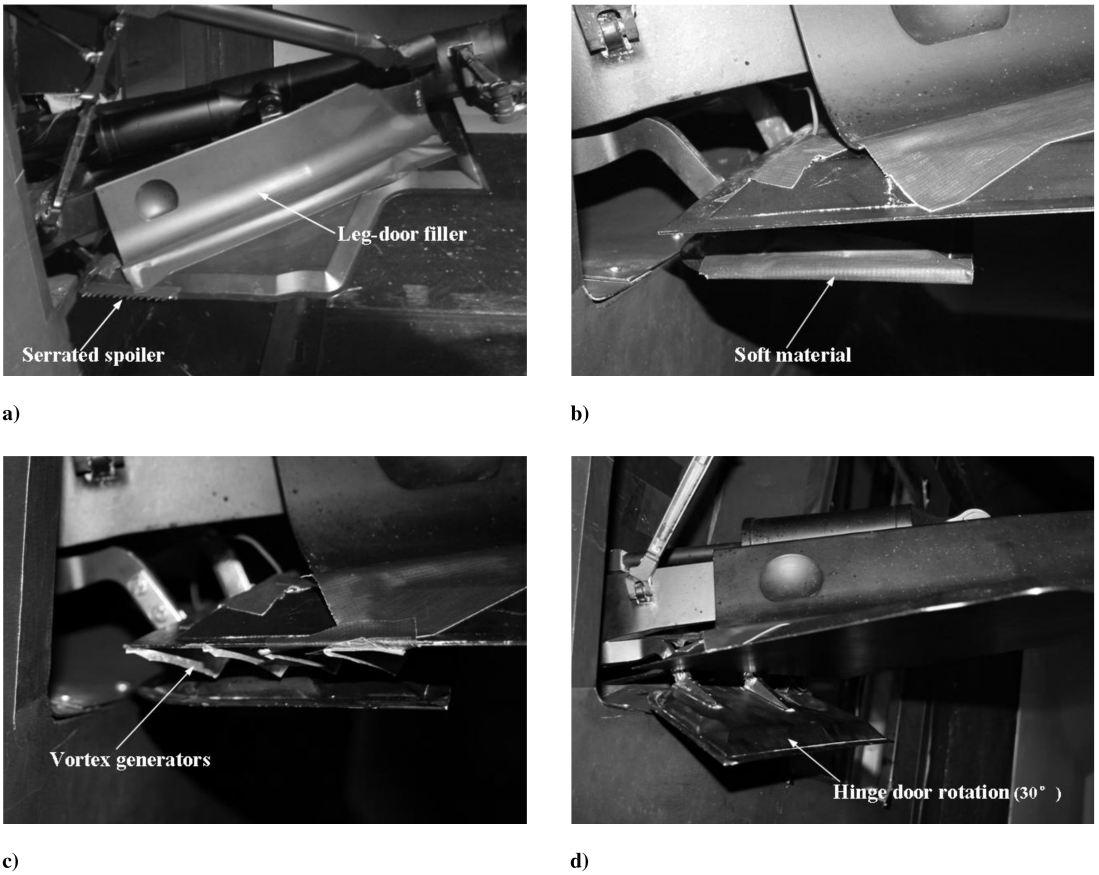

Fig. 10 Treatments for controlling the tonal noise: a) a serrated spoiler attached on the leg-door leading edge, b) soft material attached on the hinge-door leading edge, c) vortex generators mounted on the lower surface of the leg-door leading edge, and d) hinge door rotated 30 deg relative to the leg door.

The first four treatments were designed to eliminate the vortex-generating and acoustic-feedback mechanisms at the entrance to the cavity. The last treatment removed the cavity completely, so that there was no vortex feedback and no cavity resonance. The pressure fluctuations at microphone P19 on the surface of the leg door were used to determine the effectiveness of each treatment, as shown in Fig. 11. In all cases, the landing gear had the leg-door filler fairing installed, and the gear was rotated to −3 deg yaw.

Compared with the Fig. 7c, in which no control was applied, Figs. 11a, 11d, and 11e show that the serrated spoiler, the rotation of the hinge door to 30 deg, and the removal of the hinge door totally suppressed the tonal noise, because there were not any peaks in the spectra at all three measurement points. However, the other treatments of putty material on the hinge-door leading edge and the vortex generators only partially reduced the tonal-noise level, because the leading-edge P19 could still pick up some periodic pressure fluctuation (Figs. 11b and 11c).

D. Flow-Field Measurements

To further investigate the physics of the observed tonal noise and the way in which the control methods worked, the flowfield at the entrance of the cavity between the leg door and the hinge door was examined using laser PIV measurements. The only control method presented here is the serrated spoiler, which is compared with the two uncontrolled configurations, the baseline build with no leg-door filler and 0 deg yaw, and the build with the leg-door filler fairing and −3 deg yaw. Figure 12 shows the time-averaged streamwise U-velocity contours and the corresponding vectors. Flow is from left to right.

For the gear in its baseline configuration, Fig. 12a shows that there was very little recirculation in the gap area between the leading edges, and most of the flow was directed past the cavity. The flow velocity below the hinge door was much higher than the freestream wind speed of 40 m/s. When the landing gear model was rotated by a yaw angle of −3 deg and the leg-door filler fairing was installed, a strong flow recirculation in the entrance is observed, and the area of increased local flow speed below the hinge door is extended (Fig. 12b). Finally, with the serrated spoiler attached to the leg-door leading edge, the flow recirculation is slightly weaker and, importantly, the mean local flow speed below the hinge door was significantly reduced (Fig. 12c). Note that the positions of the leg door and the hinge door in Figs. 12b and 12c are slightly changed when compared with Fig. 12a due to the rotation of the landing gear.

The corresponding measured instantaneous spanwise vorticity ($\Omega_z = \partial v/\partial x - \partial u/\partial y$) of the flow is plotted in Fig. 13. Figures 13a and 13c show that discrete vortices are convected from the leg-door leading edge to the hinge-door leading edge, but for the case in which the resonance is strongly exited (in Fig. 13b), there is a continuous vortex connecting the two leading edges.

E. Far-Field Noise Test Results

Far-field noise measurements were carried out in the QinetiQ NTF test facility to verify the results from the closed-section wind tunnel. Although the serrated spoiler, the vortex generators, and the putty treatment were all effective to some extent for noise reduction in the wind-tunnel tests, they were not applied in the NTF tests, because they are not practical for real aircraft applications. Hence, only the effects of the rotation or removal of the hinge door are presented here. The hinge door was rotated by three angles of 0, 15, to 30 deg, respectively, with respect to the leg-door surface. Because of the sensitivity of the source-to-flow conditions, some initial tests were required to ensure that the resonance was actually present for a hinge-door angle of 0 deg, and the landing gear was tested with yaw angles of both 0 and −3 deg. In contrast to the wind-tunnel tests for which the tonal-noise level was much higher at a yaw angle of −3 deg than for 0 deg, in the NTF, the tonal level was almost the same for both yaw angles. This indicates slightly altered local flow conditions at the leading edges of the doors, which is to be expected because of the

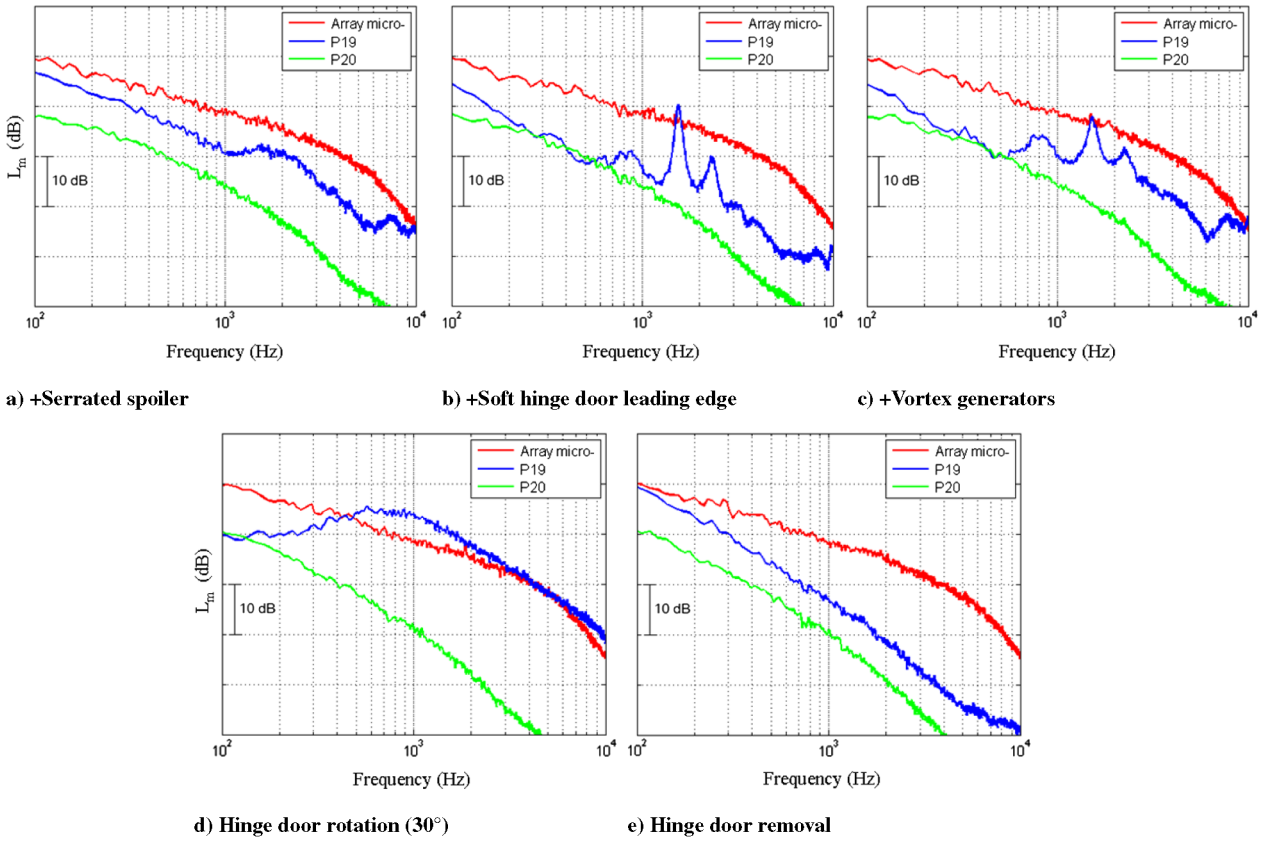

Fig. 11 Effects of the treatments on the power spectra of surface-pressure fluctuations (dB, re: 20 μ Pa) at measurement points P19 and P20 and one of the array microphones.

different wind-tunnel blockage and flow boundary conditions in the two facilities. To be consistent with the wind-tunnel tests, the subsequent testing in the NTF was carried out with a yaw angle of -3 deg.

The effect of wind speeds on the tonal noise in the NTF was monitored using the flush-mounted leading-edge microphone P19 (Fig. 14), with tests up to 78 m/s now possible. Although a number of harmonics were excited in the wind-tunnel tests, here, each spectrum contains only two dominant peaks: the driving frequency generated by the vortex feedback mechanism in the gap between the doors and the first harmonic frequency, which is amplified by the resonance of the cavity between the doors. The frequencies of the first harmonics are 1260 Hz for a wind speed of 40 m/s, 1950 Hz for 62 m/s, and 2400 Hz for 78 m/s, with the level again increasing by about 20 dB from 40 to 78 m/s. The Strouhal number of the peak is not exactly constant, being slightly lower at the highest speeds.

It is interesting to note that, for the 40 m/s test, there is a difference of about 200 Hz between the tonal frequencies in the closed wind tunnel and the NTF. The local wind speed at the doors in the closed-section wind tunnel might be expected to be higher than in the NTF tests, because the flow is constrained by the walls of the test section; although it should be noted that the area of the wind tunnel is somewhat larger than the NTF nozzle, so that the overall blockage in the wind tunnel is lower. The differences will thus be dependent upon the effective blockage in the open jet flow of the NTF, but it is worth noting that the local flow in real flight conditions is probably different

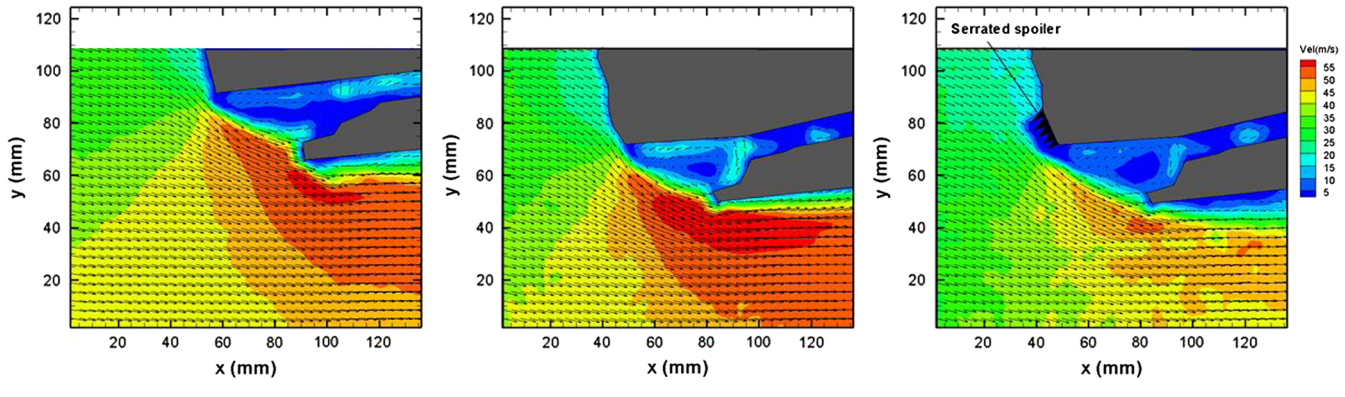

Fig. 12 Contour plots of time-averaged streamwise U velocity at the leading-edge entrance area between the leg and the hinge doors, combined with the vectors: a) baseline, without rotation; b) plus leg-door filler, with -3 deg rotation; and c) plus leg-door filler and serrated leading-edge spoiler, with -3 deg rotation. Flow is from left to right.

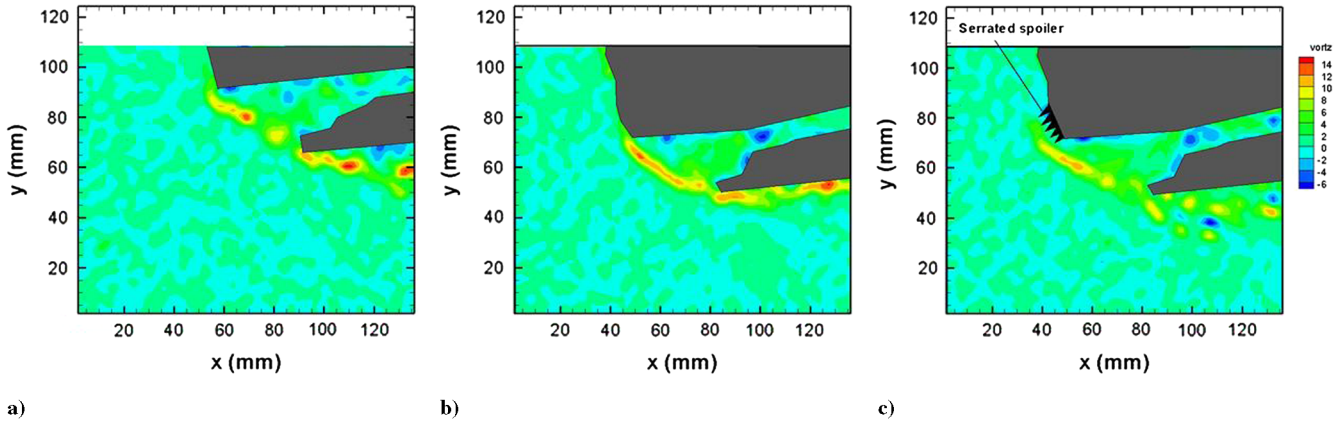

Fig. 13 Instantaneous contours of spanwise vorticity at the leading-edge entrance area between the leg and the hinge doors: a) baseline, without rotation; b) plus leg-door filler, with −3 deg rotation; and c) plus leg-door filler and serrated leading-edge spoiler, with −3 deg rotation. Flow is from left to right.

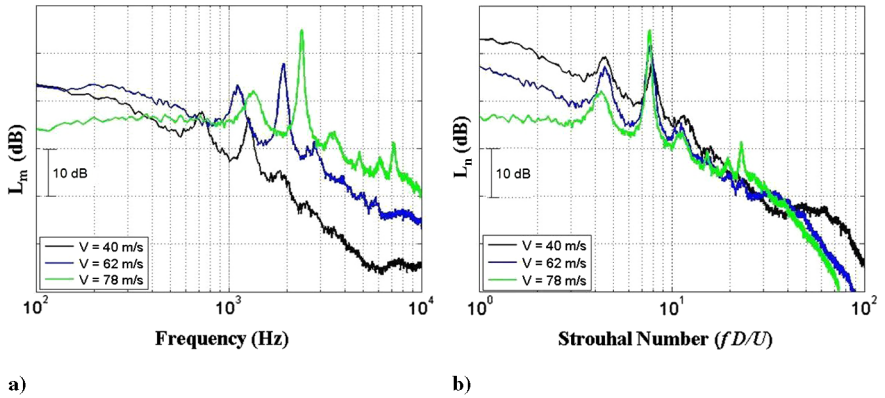

Fig. 14 Effects of wind speed on power spectra of wall pressure fluctuations at measurement point P19: a) wall pressure level vs frequency and b) normalized wall pressure level vs Strouhal number. (Hinge/leg door: 0 deg)

from both tests. The shift in frequency explains why there was a strong resonance at 40 m/s in the closed wind tunnel but not in the NTF, because the level of the second harmonic frequency depends on whether or not it coincides with a cavity resonance. At 78 m/s, the first harmonic of the driving frequency is now at 2400 Hz, and it coincides with the fifth longitudinal cavity resonance.

The effects of varying the hinge-door angle or removing the hinge door on the spectra of the surface-pressure fluctuations are shown in Fig. 15, demonstrating that the tonal noise is totally suppressed, although there was some increase in broadband pressure fluctuations.

To illustrate the effects on the far-field noise, Fig. 16 shows the narrowband noise spectrum for a hinge-door angle of 0 deg at three different polar microphones representing the forward arc (P60), the overhead (P90), and rear arc (P140) radiation direction, respectively. It is apparent that the tone was most prominent in the rear arc and was comparable with the broadband noise spectrum in the other two directions. The azimuthal variation of the tone is shown in Fig. 17, using data from three microphones on the azimuthal array with the ring positioned at a polar angle of $\Psi = 150$ deg (i.e., in the rear arc). The peak tonal noise was roughly aligned with the landing-gear leg

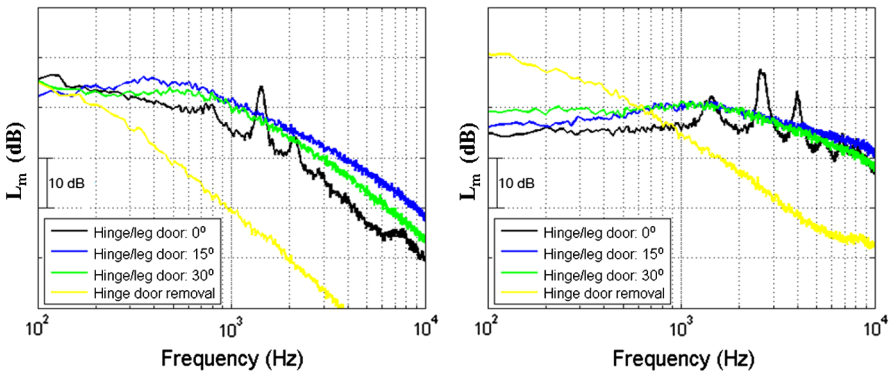

Fig. 15 Effects of noise reduction treatment on power spectra of wall pressure fluctuations at measurement point P19 for two freestream wind speeds of 40 and 78 m/s.

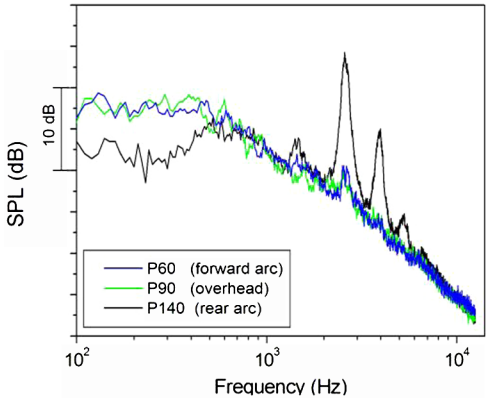

Fig. 16 Narrowband noise spectra at a wind speed of 78 m/s for three different polar angles (60, 90, and 140 deg). (Hinge/leg door: 0 deg)

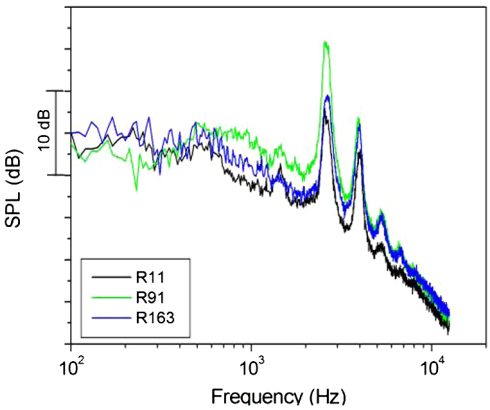

Fig. 17 Narrowband noise spectra at a wind speed of 78 m/s for three different azimuthal radiation angles (11, 91, and 163 deg) on the traversing microphone array with a polar angle of $\Psi = 150$ deg. (Hinge/leg door: 0 deg)

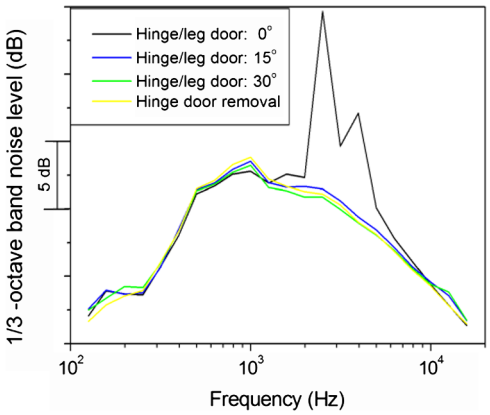

Fig. 18 Comparison of one-third-octave band spectra of microphone R91 at far field of polar angle $\Psi = 150$ deg ($U_\infty = 78$ m/s). (Hinge/leg door: 0 deg)

(i.e., the horizontal direction, here), and the tonal-noise level was about 7 dB lower at 163 deg azimuthal and 10 dB at 11 deg azimuthally.

Finally, Fig. 18 presents a one-third-octave frequency band in sound pressure level (SPL) for the different builds, showing how dominant the tone was in the NTF facility once the gear was aligned, so as to maximize the strength of the tone.

IV. Conclusions

A one-quarter-scale A340 main landing gear model was used to identify and control a source of tonal-noise that had been noted in previous projects but never fully understood. Aeroacoustic and aerodynamic measurements were made in a closed-section wind tunnel with a phased microphone array, flush-mounted microphones on the model, and the PIV technique, and in an open jet aeroacoustic facility with two far-field microphone arrays. The tonal-noise source was very sensitive to the precise yaw angle of the gear in the flow, and the gear had to be rotated a few degrees to generate a strong tone in the closed wind tunnel, although this was not necessary in the open jet facility. Microphone array measurements confirmed that the tonal-noise source was located from the general area of the leg-door and hinge-door leading edges, and a flush-mounted microphone in the gap between the doors showed high-level pressure fluctuation at the frequency of the tone.

The mechanism for the noise source has been shown to be a combination of a vortex shedding feedback in the gap between the leading edges of the doors and a resonance associated with the length of the open cavity between the two doors. Far-field data from the NTF showed that the tone was more pronounced in the rear-arc radiation direction than in the forward-arc or overhead directions.

A number of methods were used to control the tone, the most practical of which was either rotation of the hinge door, so that it was no longer parallel to the leg door, or complete removal of the hinge door.

Acknowledgments

This project was cofunded by the United Kingdom Technology Strategy Board's collaborative research and development program. The work described in the paper, including the Noise Test Facility (NTF) tests, was also cofunded by Airbus. The program for the beamforming software was supplied by Benjamin Fenech from the school of Engineering Sciences. The test data acquisition in the NTF was carried out by a team led by Richard Pinker and Andrew Bennett, and it was coordinated by Airbus.

References

[1] Crighton, D. G., "Airframe Noise," *Aeroacoustics of Flight Vehicles: Theory and Practice*, Vol. 1, NASA, 1991, pp. 391–447; also NASA RP 1258.

[2] Macaraeg, M. G., "Fundamental Investigations of Airframe Noise," AIAA Paper 98-2224, 1998.

[3] Dobrzynski, W., Chow, L. C., Guion, P., and Shiells, D., "Research into Landing Gear Airframe Noise Reduction," AIAA Paper 2002-2409, 2002.

[4] Piet, J. F., Davy, R., Elias, G., Siller, H., Chow, L. C., Seror, C., and Laporte, F., "Flight Test Investigation of Add-On Treatments to Reduce Aircraft Airframe Noise," AIAA Paper 2005-3007, 2005.

[5] Molin, N., Piet, J. F., Chow, L. C., Smith, M., Dobrzynski, W., and Seror, C., "Prediction of Low Noise Aircraft Landing Gears and Comparisons with Test Results," AIAA Paper 2006-2623, 2006.

[6] Dougherty, R. P., "Beamforming in Acoustic Testing," *Aeroacoustic Measurements*, edited by Mueller, T. J., Springer, Berlin, 2002, Chap. 2.

[7] Underbrink, J. R., "Aeroacoustic Phased Array Testing in Low Speed Wind Tunnels," *Aeroacoustic Measurements*, edited by Mueller, T. J., Springer, Berlin, 2002, Chap. 3.

[8] Fenech, B., and Takeda, K., "SotonArray: Southampton University Wind Tunnel Microphone Array System Guide," Univ. of Southampton TR 07/03, Southampton, England, U.K., 2007.

[9] Raffel, M., Willert, C., and Kompenhans, J., *Particle Image Velocimetry, A Practical Guide*, 3rd ed., Springer, Berlin, 2000.

[10] Moffat, R., "Describing the Uncertainties in Experimental Results," *Experimental Thermal and Fluid Science*, Vol. 1, No. 1, 1988, pp. 3–17. doi:10.1016/0894-1777(88)90043-X

[11] Amiet, R. K., "Correction of Open Jet Wind Tunnel Measurements for Shear Layer Refraction," AIAA Paper 75-532, 1975.

[12] Howe, M. S., *Acoustics of Fluid-Structure Interactions*, Cambridge Univ. Press, New York, 1998.

[13] Kinsler, L. E., Frey, A. R., Coppens, A. B., and Sanders, J. V., *Fundamentals of Acoustics*, 3rd ed., Wiley, New York, 1982.